Journal of Applied Polymer Science

Comparing Cracking Time and Structure Changes of Different High-Density Polyethylenes During Stress and Photo-Oxidative Aging

Zhengyu Huang, Yongliang Li, Xiancheng Ren
College of Polymer Science and Engineering, Department of Polymer Science and Engineering, Sichuan University, Chengdu 610065, China
Correspondence to: X. Ren (E-mail: xiancren@sina.com)

ABSTRACT: This article describes the structure changes of high-density polyethylene (HDPE) during stress and photo-oxidative aging experiments, and the relationship between different materials and cracking time. The three most representative grades of HDPE are 9070, TR480, and 2480NT. The average molecular weight, the comonomer type, and content of materials were measured by high-temperature gel permeation chromatography, ^{13}C nuclear magnetic resonance (NMR) spectroscopy, and successive self-nucleation and annealing technique. Moreover, tensile testing was done to distinguish different toughness of materials. The samples were exposed to 5 MPa stress and ultraviolet irradiation in an aging oven, and observed at time intervals. The changes in structure were characterized by metallurgical microscopy, differential scanning calorimetry, attenuated total reflection-Fourier transform infrared spectroscopy, X-ray diffraction, and gel content measurements. With increasing time, the crystallinity increased, whereas melting point and oxygen induction times decreased. Meanwhile, the carbonyl index values and gel content reached about 10% until the samples were cracked. The results manifested that the resistance to cracking of the different HDPEs followed the order: 2480NT > TR480 > 9070. © 2014 Wiley Periodicals, Inc. J. Appl. Polym. Sci. **2014**, *131*, 40904.

KEYWORDS: aging; degradation; irradiation; properties and characterization; thermal properties

Received 12 December 2013; accepted 25 April 2014
DOI: 10.1002/app.40904

INTRODUCTION

High-density polyethylene (HDPE) is a commercial plastic of economical significance. The material has been widely applied for pipes, fibers, rope, woven bags, fishing nets, insulation tube, and containers, because of its cold resistance, chemical stability, high rigidity, and excellent dielectric properties.[1] However, it has weak ultraviolet irradiation resistance, and it is vulnerable to crack under stress aging. So many researchers studied about photo-oxidative aging on HDPE and analyzed changes in mechanical properties and chemical structure.[2–5] On the other hand, many works discussed about stress aging on HDPE with the crack growth and predicted the lifetime of material.[6–9] Nevertheless, there are a few studies simulating materials aging under stress and photo-oxidative conditions.[10,11]

In this work, the materials were applied on an aging oven which with ultraviolet irradiation, stress, and humidity thermal conditions to simulate the HDPE materials accelerated aging process. The specimens were under a constant loading below safety stress,[12–14] which was less than 25% breaking strength of materials. High-resolution ^{13}C nuclear magnetic resonance (NMR) spectroscopy was used extensively to study the polyethylene structure and assign all the carbon resonances for branches.[15,16] Successive self-nucleation and annealing (SSA)[17–20] technique is commonly used to recognize the comonomer content of materials. Structure changes and crack propagation in the aging process were analyzed by metallurgical microscopy, differential scanning calorimetry (DSC), X-ray diffraction (XRD), attenuated total reflection-Fourier transform infrared (ATR-FTIR) spectroscopy, and gel content testing. Our aim was to determine whether a correlation exists in comonomer, toughness, and crack time of different HDPEs.

EXPERIMENTAL

Materials and Sample Preparation

The three white pellet materials, 9070, TR480, and 2480NT, were supplied by Hanwha Chemical Corp., Sinopec Maoming Petrochemical, and Dow Chemical, respectively. Antioxidant Irganox 1010 and auxiliary antioxidant 168 were procured from Ciba Specialty Chemicals (Switzerland). The parameters of the three materials are shown in Table I. Average molecular weights and molecular weight distributions were tested by high-temperature gel permeation chromatography (PL-GPC220, Polymer Laboratories, England).

Three kinds of samples were prepared by mixing and extruding HDPE with 2.5 wt ‰ antioxidant Irganox 1010 and 2.5 wt ‰ auxiliary Irganox 168 in a twin-screw extruder (TSSI-25,

Table I. Some Samples Characteristics

Sample	Density (g cm^{-3})	M_n (kg mol^{-1})	M_w (kg mol^{-1})	M_w/M_n
9070	0.945	175	199	1.14
TR480	0.944	41.3	43.8	1.06
2480NT	0.949	33.2	44.3	1.33

ChenGuang Chemical Research Institute of Plastic Machinery, China) at 195°C–200°C. Sheets with a thickness of 2.1 mm were then processed by compression molding the extruded three samples for 20 min at 190°C and 10 MPa in a molding test press (XLB, Qingdao Dongya Rubber Machine Group Co.). Afterward, sheets were allowed to cool down and were then cut into dumbbell-shaped specimens for aging experiments and tensile testing according to the Chinese standard GB11997-89. Dumbbell-shaped specimens had a length of 120 mm and a width of 25 mm.

Aging Condition

Stress and photo-oxidative aging experiments were carried out in a homemade aging oven (Chengdu Yibang Analysis Instrument Co.) at 50°C ± 2°C with air circulation and relative humidity of 30% ± 2%. The specimens were applied 5 MPa stress in the oven, which was equipped with a 1000 W Ga–In source lamp. The spectrum range of lamp was 300–405 nm, with a maximum intensity at 365 nm. The irradiation intensity was 3.5 W m^{-2} tested by an UV irradiance meter model UV-A tester (Photoelectric Instrument Factory of Beijing Normal University, Beijing, China). The UV-A tester used a 365 nm probe, and the measured spectrum range was 320–400 nm. Specimens were withdrawn from the oven to observe at time intervals. Then specimens were analyzed by metallurgical microscopy, ATR-FTIR spectroscopy, DSC, XRD, and gel content measurement.

Characterization

NMR Spectroscopy. HDPEs were dissolved in 1,2-dichlorobenzene, and their ^{13}C NMR spectra were obtained with Bruker Avance AV II-600 MHz (^{13}C, 150.9 MHz) at 125°C. All ^{13}C spectra were acquired under complete proton decoupling, and chemical shift was referenced to external tetramethyl silane.

Successive Self-Nucleation and Annealing Technique. The SSA analysis comprised of successive heating and refrigerated cooling programs operating on a TA instrument DSC Q200 under a rate of 50 mL min^{-1} N_2 flow. The self-nucleation and annealing temperatures (T_s) were determined by Fillon et al.[21]

The samples were heated from 30°C to 200°C, and then maintained for 5 min to erase the thermal history. Afterward, samples were cooled to 30°C for creating an initial standard thermal history. Then, samples were heated to the first self-nucleating annealing temperature ($T_{s,1}$) of 132°C, and maintained for 60 min with modulation amplitude of ±1°C and modulation period of 100 sec, and then cooled to 30°C. The samples were heated again to $T_{s,2}$ of 128°C and treated for 60 min under the same amplitude and period modulation, and then cooled to 30°C. This cyclic treatment was continued with the $T_{s,n+1}$ being 4°C lower than $T_{s,n}$, and the last one, $T_{s,12}$, was 88°C. The heating and cooling rates were both 10°C min^{-1}. The ultimate heating curves were gotten by heating the samples from 30°C to 200°C at a rate of 5°C min^{-1}, which reflected the multiple melting peaks.

Tensile Testing. The tensile properties of materials were characterized by an AGS-J tensile testing machine (Shimadzu, Japan) with a 10-kN load cell, operating at a cross-head speed of 50 mm min^{-1}, according to Chinese standard GB/T1040–1992. The software provided calculates average values after measuring five specimens of each sample.

Metallurgical Microscopy Observations. Metallurgical microscopy observations were applied on a UM200i metallurgical microscope (Chongqing UOP Photoelectric Technology Corp., China) for detecting the surface of specimens during stress and photo-oxidative aging.

Fourier Transform Infrared Spectroscopy. ATR-FTIR spectroscopy was measured by a Nicolet 6700 instrument equipped with a diamond ATR accessory. Carbonyl index (CI) value was obtained from the carbonyl stretching area peak area (1670–1800 cm^{-1}) and CH_3 stretching peak band area (2917 cm^{-1}). CI was determined as follows:

$$CI = \frac{A_{C=O}}{A_{2917}} \quad (1)$$

Here $A_{C=O}$ and A_{2917} are, respectively, carbonyl group absorption peak areas and internal reference peak areas.

Differential Scanning Calorimetry. The TA instrument DSC Q200 was used for the thermal analysis of specimens processed at different aging times. Approximately, 5 mg powder samples scraped from the surface of specimens were heated from 40°C to 210°C, at a rate of 10°C min^{-1}. The heat of fusion (ΔH) of experimental melting peak area was derived to calculate crystallinity (X_c):

$$X = \frac{\Delta H}{\Delta H_{100}} \times 100\% \quad (2)$$

Here ΔH_{100} is defined as the heat of fusion of 100% crystalline HDPE (293 J/g[22,23]).

In addition, oxidation induction time (OIT) was measured on the same instrument. Five milligrams of samples were heated to 210°C at the same rate, with 50 mL min^{-1} N_2 flow. After thermal equilibration for 5 min, the purge gas was switched to O_2. OIT is the time interval between O_2 insertion and oxidation onset point measured within ±0.1 min.

X-ray Diffraction Characterization. Crystal characterization of HDPE specimens was carried out on XRD (X'Pert Pro MDP, Royal Dutch Philips Electronics Ltd.). The measurements were performed in reflection mode with Cu Kα radiation (40 kV, 35 mA), $\lambda = 1.5418$ Å.

Gel Content (Crosslinking Degree) Measurement. According to ASTM D 2765, a continuous extraction experiment was performed in 350 mL xylene solvent with 1 wt % Irganox 1010 for 12 h at 110°C. Approximately, 0.300 ± 0.015 g sample was cut into small pieces and placed in a preweighed 120-mesh stainless

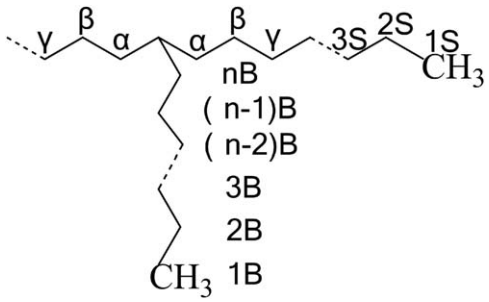

Figure 1. Carbon numbering scheme for short-branched HDPE.

steel cloth pouch. After extraction, sample was immediately placed in a cage in a vacuum oven and heated to 150°C until a constant weight was reached. The gel contents were calculated using the following equation:

$$\text{Gel content}\ (\%) = 100\% - \frac{W3 - W4}{W2 - W1} \times 100\% \qquad (3)$$

Here, $W1$ is the weight of the pouch, $W2$ is the weight of the sample and the pouch, $W3$ is the weight of the cage, and $W4$ is the constant weight of the cage.

RESULTS AND DISCUSSION

Characterization of Unaged Samples

^{13}C NMR. A general structure for short chain branches in polyethylene is shown in Figure 1, and carbons were named based on Randall.[24] The ^{13}C NMR spectra of three samples are shown in Figure 2. The assignment of each peak was labeled across the top of each HDPE spectrum, and the ^{13}C chemical shift values of various carbons are listed in Table II. From Table II we found out that the shift value of each carbon was similar. The average molecular weight of 9070 was much higher than the other two; so, the intensity of peaks in ^{13}C NMR spectrum was larger. Then according to Grant–Paul chemical shift rules,[25] Lindeman–Adams methods,[26] and the spectra of model copolymers,[27] this confirmed that the short chain branch present was butyl. From the above analysis we can conclude that the comonomer type of all the three samples was 1-hexene.

Thermal Fractionation. Thermal fractionation SSA is the most powerful and effective technique for the characterization of polyolefin comonomer content. Figure 3 revealed the ultimate DSC heating curves after SSA of three unaged HDPE samples. Multiple melting peaks were formed during each step of self-nucleation and annealing crystallization, and the peaks fitting curves are shown in Figure 4. Each step of endotherm peak region represents a series of crystals, which had almost the same

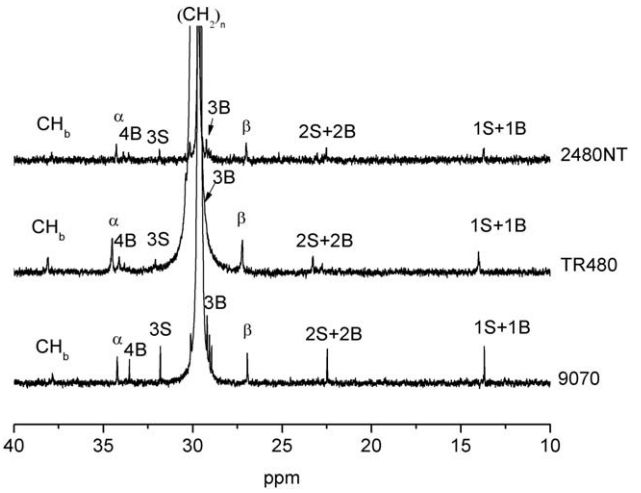

Figure 2. ^{13}C NMR spectra of three samples showing detailed branch assignments.

thermodynamic stability and melting temperature, and the differences among the peaks were mostly caused by different crystal sizes.[28]

The thickness of the crystal lamellae (l_i) can be determined by DSC melting point of the polymer via the Thomson–Gibbs equation (eq. (4)).[17]

$$l_i = \frac{2\sigma_s Tm^0}{\Delta Hv(Tm^0 - Tmi)} \qquad (4)$$

By the Keating[18] method and Flory[20] equation, mathematical calibration relationship was obtained based on between the melting point and the methylene sequence length (MSL)[29]:

$$-\ln(CH_2\ \text{mole fraction}) = -0.31767 + \frac{131.61}{T_{mi}} \qquad (5)$$

CH_2 mole fraction represented the corresponding peak region of the methylene content; further the CH_3 mole fraction was obtained. MSL can be calculated by the following formula (eq. (6)):

$$MSL = \frac{2(CH_2\ \text{mole fraction})}{1 - (CH_2\ \text{mole fraction})} \qquad (6)$$

Meanwhile, the comonomer content of each segment can be obtained by multiplying the peaks area with its corresponding ratio.[19]

Arithmetic mean $\overline{L_n}$, weighted mean $\overline{L_w}$, and sequence length broadness index I were determined from following equations[19–21,29,30]:

Table II. ^{13}C Chemical Shift Values of Various Carbons in HDPE Main Chain and Side Chain

	Main chain (ppm)						Side chain (ppm)			
Sample	CH	α	β	1S	2S	3S	1B	2B	3B	4B
9070	37.9	34.2	26.9	13.7	22.5	31.8	13.7	22.5	29.1	33.5
TR480	38.1	34.5	27.2	14.0	23.3	32.1	14.0	23.3	29.9	34.1
2480NT	37.9	34.3	27.0	13.8	22.6	31.9	13.8	22.6	29.2	34.0

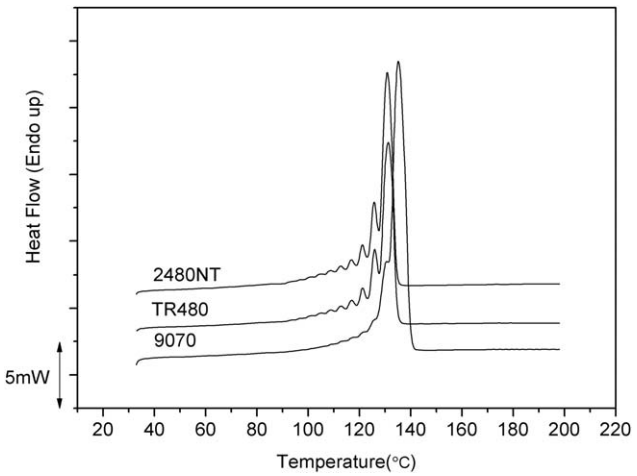

Figure 3. Final heating curves after thermal fractionation of three samples of HDPE.

$$\overline{L_n} = \frac{n_1 L_1 + n_2 L_2 + \cdots + n_j L_j}{n_1 + n_2 + \cdots n_j} = \frac{n_1}{N} L_1 + \frac{n_2}{N} L_2 + \cdots + \frac{n_j}{N} L_j = \Sigma f_i L_i \tag{7}$$

$$\overline{L_w} = \frac{n_1 {L_1}^2 + n_2 {L_2}^2 + \cdots + n_j {L_j}^2}{n_1 L_1 + n_2 L_2 + \cdots + n_j L_j} = \frac{\Sigma f_i {L_i}^2}{\Sigma f_i L_i} \tag{8}$$

$$I = \frac{\overline{L_w}}{\overline{L_n}} \tag{9}$$

Here n_i is each segment of the normalized peak area, and L_i is each segment of MSL or lamellar thickness for each fraction. By using these equations, we determined the polydispersity parameters in Table III.

The differences among the samples were qualitatively displayed by the number and area of melting peaks in heating curves. The curves in Figure 3 were existed more obvious thermal fractionation melting peaks in TR480 and 2480NT, whereas 9070 was of the highest temperature peak. Besides, the curve of TR480 was similar with that of 2480NT due to a few differences in melting peaks in Figure 3. The results in Table II could explain the similarity between TR480 and 2480NT, attributed to the almost same comonomer content, mean sequence length, and average lamellar thickness in Table III. 9070 had the lowest comonomer content (0.75 mol %), the longest mean sequence length (391.81), and the maximum average lamellar thickness (29.65 nm); meanwhile, the I_L(1.29) and I_l(1.26) were highest. It demonstrated that the comonomer content of sample was lesser, and the longer MSL renders molecular chains arrangement tidier. At the same time, the molecular chains easily moved into the crystal lattice, making the crystallization ability of sample stronger, and results in lamellar thickness becomes thicker.

Mechanical Properties Analysis. The mechanical properties tests of HDPE specimens were carried out to determine tensile strength, breaking strength, elongation, and fracture toughness on the tensile testing machine.

Fracture toughness is the area under stress–strain curve, the work done on the material from start to fracture. Table IV shows that the breaking strength and fracture toughness of 9070 samples were the lowest, whereas 2480NT samples had the highest breaking strength (34.63 MPa) and fracture toughness (208.28 J). The results can be explained with average molecular weights and molecular weight distribution of samples in Table I. The 9070 had the biggest average molecular weight and narrowest molecular weight distribution. M_n of 2480NT (33.2 kg mol^{-1}) was smaller than that of TR480 (41.3 kg mol^{-1}), and M_w/M_n (1.33) of 2480NT was broader. Consequently, there were many low-molecular-weight chains in 2480NT, which can provide flexibility in tensile testing period. As the comonomer of three samples was 1-hexene, the degree of short chain branch depended on comonomer content. Therefore, 2480NT had the highest degree of short chain branch; it made the distance between molecule chains to increase and the intermolecular forces to reduce. So, 2480NT had the excellent toughness compared with other two.

Stress and Photo-Oxidative Aging of Samples

Surface Morphology Observation. The surfaces of three HDPE samples were observed with metallurgical microscopy. The micrographs at a magnification of 100 times are displayed in Figure 5. Direction of the arrows in Figure 5(a) was the 5 MPa stress direction and was the same for other samples. The micrographs in Figure 5(a,d,g) showed that the non-aged samples were smooth, without any cracks.

From Figure 5(b,e,h), we found that the surface of 9070 and TR480 samples were not with obvious microcracks like 2480NT. After 250 h of stress and photo-oxidative aging, the crack width was about 10 μm in Figure 5(c,f). However, the crack density of 9070 was larger than that of TR480 samples; also, fracture phenomena occurred on 9070 samples because of more defects. Figure 5(h) shows that in 2480NT samples microcracks appeared after 300 h of aging. Then 12–14-μm width cracks appeared

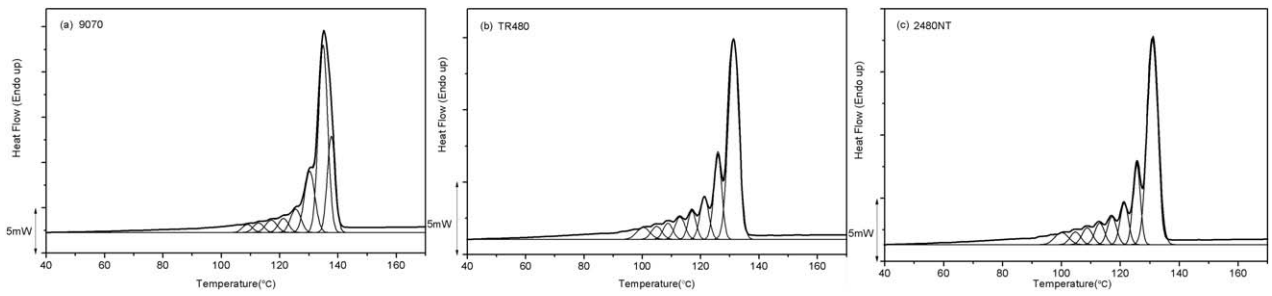

Figure 4. Peak fitting curves of thermal fractionation curves for three samples: (a) 9070, (b) TR480, and (c) 2480NT.

Table III. Parameters of Thermal Fractionation for Three Samples of HDPE

Sample	MSL			*l*(nm)			Comonomer content (mol %)
	$\overline{L_n}$	$\overline{L_w}$	I_L	$\overline{l_n}$	$\overline{l_w}$	I_l	
9070	391.81	504.99	1.29	29.65	37.45	1.26	0.75
TR480	190.18	219.93	1.16	14.99	17.12	1.14	1.31
2480NT	186.51	213.87	1.15	14.72	16.68	1.13	1.32

Table IV. Three Kinds of HDPE Mechanical Properties

Sample	Tensile strength (MPa)	Breaking strength (MPa)	Elongation (%)	Fracture toughness (J)
9070	26.98	21.17	681.26	157.49
TR480	20.27	33.70	783.82	202.11
2480NT	21.24	34.63	696.43	208.28

after 350 h aging [Figure 5(i)]. At the same time, the direction of crack propagation was vertical to the stress direction on the surface of all samples.

When the three kinds of HDPE were subjected to long-period stress and ultraviolet irradiation aging, 9070 was the first to crack and fracture, which validated that 9070 has the weakest stability and is more susceptible to crack on aging degradation. On comparing the cracking time of the three materials, the following order was seen: 2480NT > TR480 > 9070.

Changes in Solid-State Structure of HDPE Samples after Aging. In principle, the changes in solid-state structure and chemical structure occurred due to aging, such as changes in molecular weight or branch formation and crosslinking could induce changes in crystallization and melting behavior that would be recorded by DSC technique.

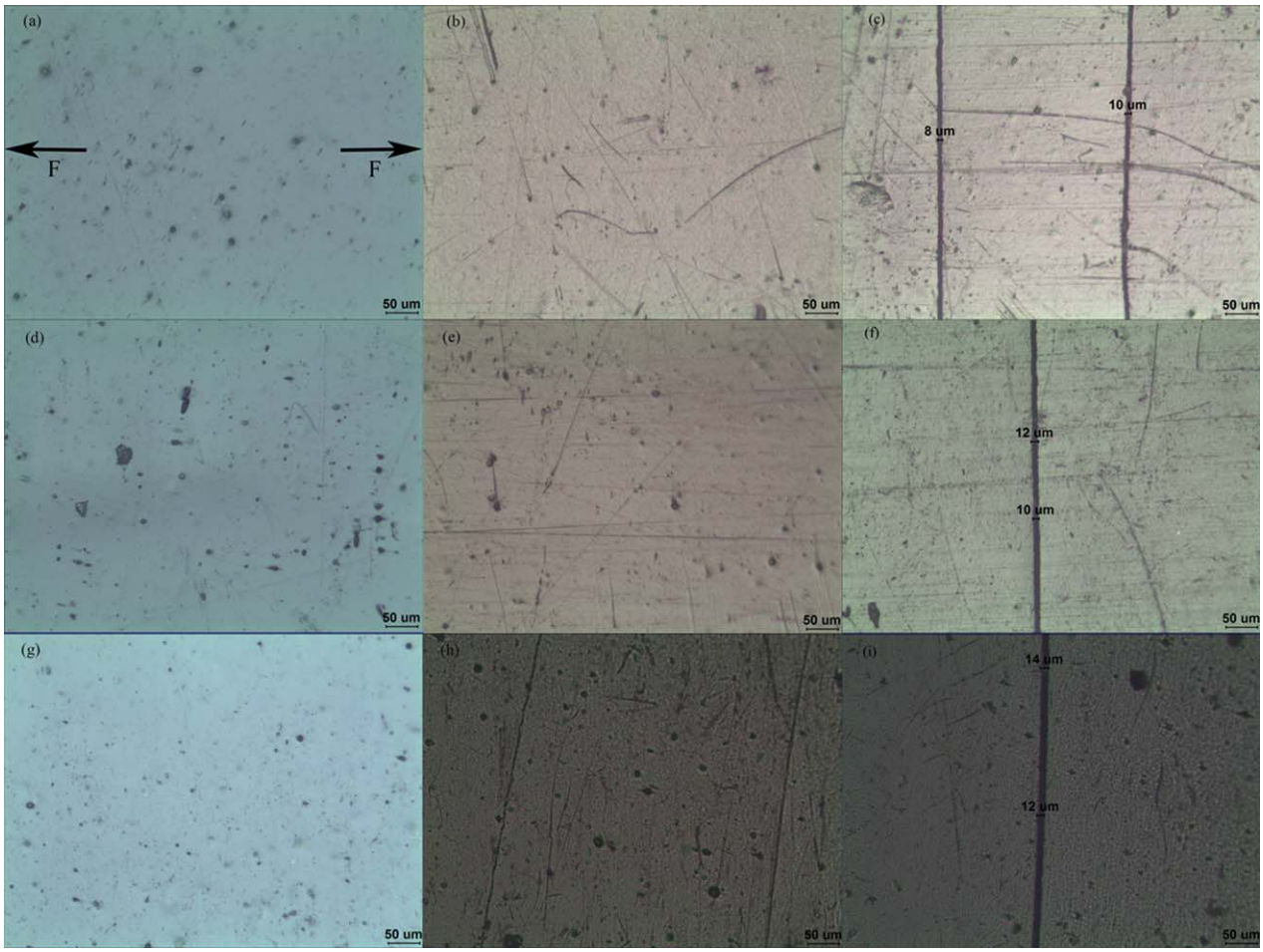

Figure 5. Micrographs of three sample surfaces during stress and photo-oxidative aging. 9070: (a) 0 h, (b) 225 h, and (c) 250 h. TR480: (d) 0 h, (e) 225 h, and (f) 250 h. 2480NT: (g) 0 h, (h) 300 h, and (i) 350 h. [Color figure can be viewed in the online issue, which is available at wileyonlinelibrary.com.]

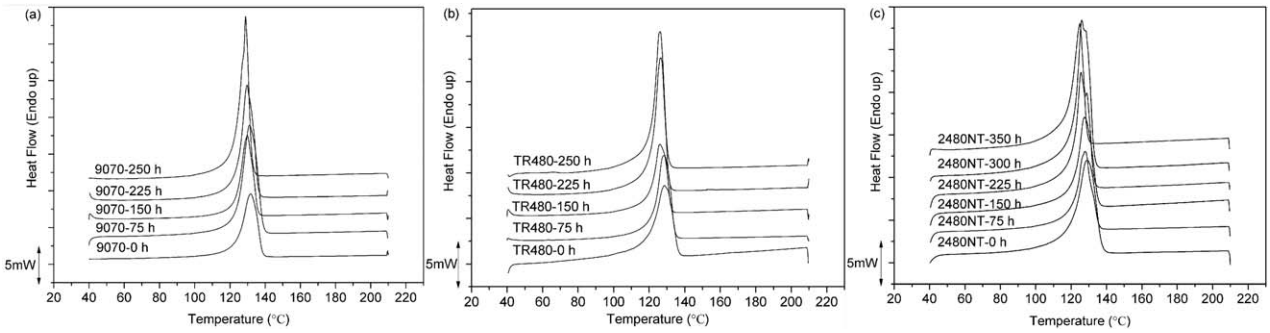

Figure 6. DSC crystallization curve of three samples of HDPE during stress and photo-oxidative aging: (a) 9070, (b) TR480, and (c) 2480NT.

Figure 6 shows the DSC thermograms for samples under different aging times. The most relevant data are summarized in Table V. From Figure 6, the melting peak area of each HDPE sample became larger and melting point slightly shifted to the right with aging time increasing. As it could be seen in Table V, the X_c of 9070 grew from 47.94% to 61.09% till cracking, X_c of TR480 increased from 36.96% to 49.76%, and X_c of 2480NT also increased from 37.55% to 52.59%. The T_m of HDPE reduced with increasing aging time; for 9070 and TR480, it decreased about 3°C, and the T_m of 2480NT decreased approximately 4.3°C. OIT tests were used to determine the materials' stability during aging. With increasing time, OIT of all samples reduced to nearly 1 min.

Besides, the crystallinity and melting point values of the unaged 9070 sample were the biggest, consistent with that of the thermal fractionation results. After 250 h of aging, 9070 fractured, but only some cracks appeared on the aged surface of TR480; it may be because its crystallinity was higher than that of TR480. Due to the crystallinity increasing slowly and the OIT decreasing slowly, so 2480NT finally appeared cracks.

Sabino et al.[31] reported that the longest chain segments had a high probability of being entangled within the amorphous regions, which were regions vulnerable to degradation, and then tie-molecules and entangled chains of long MSL segments would have a high possibility of being involved in degradation reactions. Thus, our result about the cracking time order is in agreement with this theory; the long MSL chain segment of the 9070 sample was more susceptible to degradation. Carrasco et al.[3] suggested that the UV irradiation had a little influence on crystallinity during HDPE aging. Due to tensile 5 MPa stress, HDPE chain segments were prone to orientation or recrystallization in the stretching direction. In addition, the temperature of the sample surface was 55°C, which was higher than the glass-transition temperature, so it was advantage for chain movement and rendering chains arrange more closely. So the degree of crystallization of HDPE samples increased during stress and photo-oxidative aging. It illustrated that the three materials' crystallinity added about 15%, and the samples became brittle and cracked after aging. At the same time, the T_m of materials decreased; it showed that some small molecule chains were produced, and partial degradation of the material occurred in the aging process, which were mainly manifested in chain scission and chain break. Besides, the OIT for three materials reduced to 1 min, which could describe that the surface of samples had been part of oxidation that results would be found in Figures 6 and 7. As irradiation time increased, the samples surface gradually turned yellow and became brittle, which made the material to more quickly degrade and ultimately accelerated the aging process.

Chemical Changes on the Surface of HDPE Samples after Aging. IR spectroscopy was widely used to determine the presence of various oxidation products that were formed as a result of polyethylene samples degradation reactions.[32–34] In our context, ATR-FTIR spectroscopy characterized the chemical changes

Table V. Crystallinity, Melting Point, and OIT of Three Samples on Different Aging Times

	Samples								
	9070			TR480			2480NT		
Time (h)	X_c (%)	T_m (°C)	OIT (min)	X_c (%)	T_m (°C)	OIT (min)	X_c (%)	T_m (°C)	OIT (min)
0	47.94	131.85	95.07	36.96	128.64	34.09	37.55	129.17	47.04
75	54.66	131.14	2.03	43.98	128.32	2.07	39.65	127.81	1.86
150	55.05	129.84	2.02	43.10	125.91	1.63	42.35	127.59	2.22
225	58.45	129.76	1.58	47.03	126.26	1.21	48.57	125.58	1.68
250	61.09	128.84	1.02	49.76	126.29	0.91	-	-	-
300	-	-	-	-	-	-	52.39	125.98	1.63
350	-	-	-	-	-	-	52.59	124.87	0.88

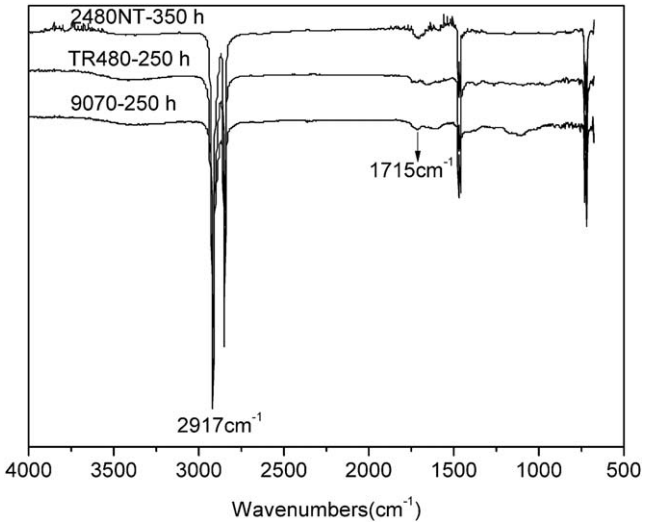

Figure 7. The ATR-FTIR spectra of three different cracked samples.

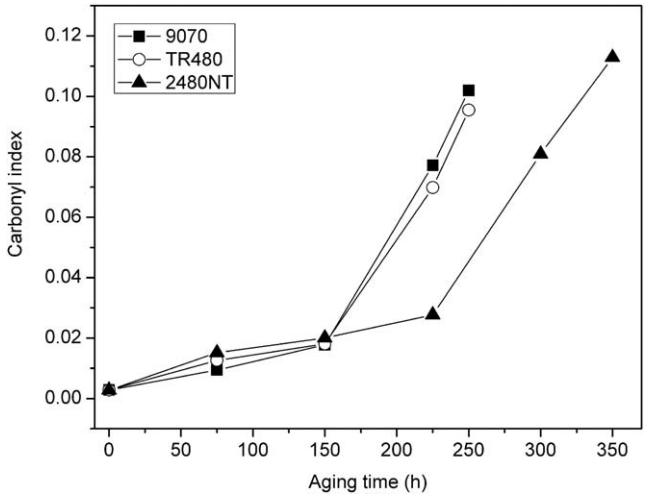

Figure 8. Changes in carbonyl index for three samples during stress and photo-oxidative aging.

on the surface of samples after aging. Figure 7 showed the ATR-FTIR spectra of the crack HDPE samples. The 2917 and 2848 cm^{-1} peaks were CH_2 asymmetric stretching and stretching vibration. The 1472 and 1462 cm^{-1} peaks were CH_2 in-plane bending and wagging vibration of the HDPE chains. The 730 and 719 cm^{-1} peaks belonged to C—H out-of-plane bending vibration. The absorption band around 1715 cm^{-1} was assigned to the C═O stretching vibration. From the ATR-FTIR spectra and the surface micrographs in Figure 5, it can be seen that the carbonyl peaks obviously appeared when the samples crack.

The CI characterized the degree of oxidation for each HDPE sample during aging. The results for three materials after different aging times are shown in Figure 8. As the time extended, CI increased significantly. The 9070 samples fractured in 250 h; the CI was 0.102. In TR480, cracks appeared after 250 h of aging; the CI was 0.096. Moreover, in 2480NT a few microcracks appeared after 300 h of aging. The CI was 0.809, and then it rapidly increased to 0.128 due to many cracks on the surface of samples after 350 h.

CI increased with aging time. It demonstrated that the materials undergo gradual oxidation reaction to produce more free radicals and chemical changes. Thus, the materials were more prone to degradation and more susceptible to molecular chain scission and chain break under aging process, rendering the flaws to appear on the surface of sample. Also Singh[35] reported that oxygen diffused faster into amorphous polyethylene regions than crystalline regions. So based on the above analysis, it was easier for oxygen to penetrate inside via the flaws, making the materials more sensitive to degradation. Besides the appearance of crack on samples, CI values reached about 10%. The oxidation rate was in the following order: 9070 > TR480 > 2480NT, which was in line with surface observations and DSC analyses.

Changes in Crystalline Morphology of HDPE Samples after Aging. According to the theory of X-ray diffraction method, the crystallite size was measured, and the relationship was provided by Scherrer $L_{hkl} = \frac{k\lambda}{\beta \cos\theta}$.[36] β was defined as half high of diffraction peak width (FWHM), and crystal shape factor was k (0.9).

Figure 9 showed X-ray diffractograms of three materials during stress and photo-oxidative aging. The parameters are summarized in Tables VI, VII, and VIII. As can be seen, the crystal form of the materials was still the orthorhombic system which did not change during aging, and the crystalline peaks mainly consisted of (1 1 0) and (2 0 0) reflections. It was found that there were almost few changes on (2 1 0) and (0 2 0) crystal planes, and their intensity always were very low. Apparently, there were also not many changes in the d-spacing belonging to

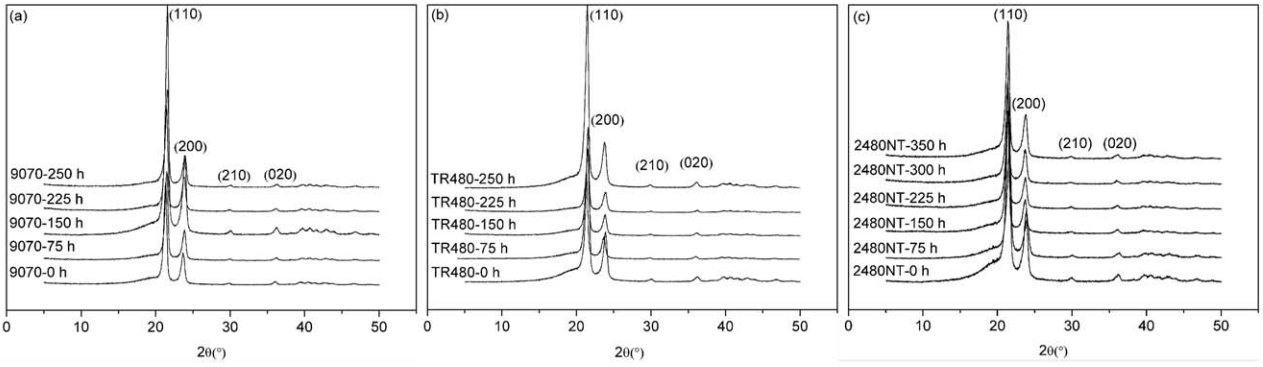

Figure 9. X-ray diffractograms of three samples of HDPE during stress and photo-oxidative aging: (a) 9070, (b) TR480, and (c) 2480NT.

Table VI. XRD-Related Parameters of 9070 on Different Aging Times

	d (Å)		Intensity (counts)		FWHM (degree)		*L* (Å)	
Time (h)	(110)	(200)	(110)	(200)	(110)	(200)	(110)	(200)
0	4.1623	3.7603	3918	1248	0.444	0.549	185	149
75	4.1389	3.7278	3407	1188	0.441	0.537	186	152
150	4.1183	3.7157	8774	2991	0.447	0.579	184	141
225	4.1409	3.7340	3926	1353	0.456	0.562	180	145
250	4.1236	3.7246	3698	1224	0.457	0.587	179	139

Table VII. XRD-Related Parameters of TR480 on Different Aging Times

	d (Å)		Intensity (counts)		FWHM (degree)		*L* (Å)	
Time (h)	(110)	(200)	(110)	(200)	(110)	(200)	(110)	(200)
0	4.1258	3.7218	8158	2706	0.474	0.596	173	137
75	4.1717	3.7591	4634	1217	0.458	0.579	179	141
150	4.1335	3.7281	4647	1138	0.455	0.593	180	137
225	4.1296	3.7248	3116	1093	0.479	0.601	171	135
250	4.1413	3.7479	9785	2446	0.462	0.630	177	129

(1 1 0) and (2 0 0) crystal planes. Due to the crystalline peak area was related with crystal content,and the crystal content was increased with crystalline peak area and FWHM. So when the FWHM was greater, it indicated that the crystal content was bigger, but rather the crystallite size became smaller.

The crystallite sizes of (1 1 0) and (2 0 0) crystal planes for 9070 samples were a bit bigger than other two samples during aging. This result was in accordance with SSA analysis, and the average lamellar thickness of 9070 was larger. It was more beneficial to the long chain segment into the lattice because of excellent crystallization performance; thus, the crystallite size of 9070 was larger than that of the other two.

As the time increased, crystallite size of all samples increased first and then decreased. It was attributed to the small molecule chains scission and breaking under stress and high temperature, which would induce the materials secondary recrystallization to render the crystallite size increase in the early period of aging process. Further the damage of (1 1 0) and (2 0 0) crystal planes and generation of crystalline imperfections after ultraviolet irradiation, mutually influenced the change in crystallite size.

Changes in Crosslinking Degree for HDPE Samples after Aging. Because of polyethylene crosslinking part did not dissolve in hot xylene, we used the ASTM D 2756 to measure the crosslinking degree for HDPE samples during aging. The crosslinking part residues weight percentage of the original sample weight was gel content that was called crosslinking degree calculating by eq. (3).

Figure 10 showed the changes of crosslinking degree for three materials during aging. The gel content of 2480NT sample was 17.76% after the longest time of 350 h. However, the crosslinking degree of the other two materials was about 10% after 250 h aging. From Figure 10, we could see that the crosslinking degree of 9070 sample was the most quickly grown to 10.53% in 250 h. For the 2480NT samples, the degree of crosslinking was rising rapidly in the aging late period. Meanwhile, crosslinking degree was 9.76% for 2480NT sample on 300 h, lower than that of 9070 and TR480 samples on 250 h. There were some relevant changes in cracking time of three materials; 9070 and TR480 were the earlier to fracture and crack.

Degradation and crosslinking were competition reactions in the aging process. Figure 11 illustrated the process of molecular

Table VIII. XRD-Related Parameters of 2480NT on Different Aging Times

	d (Å)		Intensity (counts)		FWHM (degree)		*L* (Å)	
Time (h)	(110)	(200)	(110)	(200)	(110)	(200)	(110)	(200)
0	4.1295	3.7294	6689	2126	0.478	0.618	171	132
75	4.1182	3.7066	3353	1177	0.596	0.665	136	122
150	4.1619	3.7511	3579	1013	0.472	0.618	173	132
250	4.1507	3.7419	2865	948	0.484	0.583	169	140
300	4.1582	3.7526	2993	1039	0.485	0.596	168	137
350	4.1523	3.7431	4050	1325	0.489	0.627	167	130

chains crosslinking, chain scission, and chain fracture. In our context, the result was easily concluded that crosslinking degree of all samples was increased. So the crosslinking phenomenon was more easily produced with irradiation time rising, which is shown in Figure 11(a,b). Uneven distribution of short branch chains and some molecular chains flaws lead to the irregular distribution of crosslinking segments of HDPE under UV irradiation. In combination, with our results, crosslinking degree was more than 10% and would form nonuniform network chain segments in Figure 11(b). So that the entanglements between the chain segments became fewer, resulting in poor chain segment mobility. Moreover, the chain segments hardly transfer stress, and produced stress-concentration points. So it made the molecule chains scission and break, easily leading to the materials to crack [illustrated in Figure 11(c)]. Once the crack appears on the surface of samples, it was more easy for oxygen and ultraviolet to permeate inside the materials. Besides irradiation would reduce activation energy of radicals to generate more chemical reactions, resulting in molecular chains collapse; the materials failure finally.

CONCLUSION

Three most commercially available HDPE grades under stress and photo-oxidative aging were systematically studied, and the comonomer of the materials was 1-hexene. The comonomer content, toughness, and cracking time for the different HDPEs complied with the following order: 2480NT > TR480 > 9070.

DSC analysis showed that melting point decreased about 2°C–4°C, crystallinity increased about 15%, and OIT reduced to nearly 1 min. Also, CI values of the cracking samples reached 10%. Besides (1 1 0) and (2 0 0) crystal planes were damaged, it would form a network chain segments when crosslinking degree was more than 10%. It was illustrated that three materials happened degradation and crosslinking phenomena, according to melting point were decreased and crosslinking degree of samples were increased via above analysis.

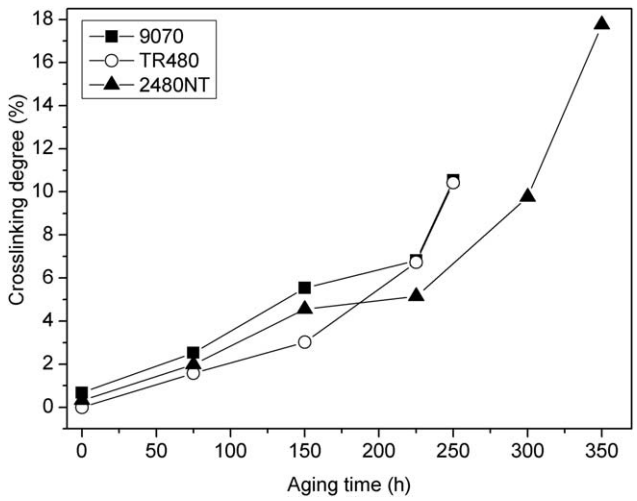

Figure 10. Changes in crosslinking degree for three samples during stress and photo-oxidative aging.

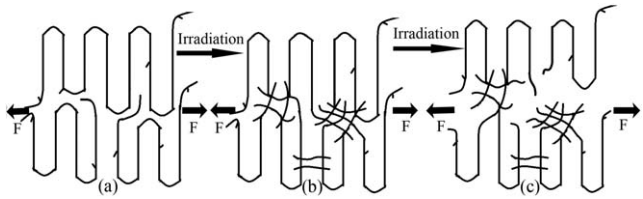

Figure 11. Schematic showing the changes in molecule chains under stress and photo-oxidative aging.

Because the materials were under stress, it would induce small molecule chains scission and breaking. Also, under ultraviolet irradiation, the chain segments mobility became poor due to crosslinking. Stress and ultraviolet irradiation mutually affected the materials, which made the HDPE crack and fracture. So according to the toughness of different HDPE materials, we can choose the best one whose average molecular weight and molecular weight distribution are moderate for outdoor applications.

ACKNOWLEDGMENTS

The authors express their great thanks to the National Natural Science Foundation of China (grant 51273130) for financial support of this work.

REFERENCE

1. Wu, S. S.; Zhang, J.; Xu, X. *Polym. Int.* **2003**, *52*, 1527.
2. Shi, X. M.; Wang, J. D.; Stapf, S.; Mattea, C.; Li, W.; Yang, Y. R. *Polym. Eng. Sci.* **2011**, *51*, 2171.
3. Carrasco, F.; Pages, P.; Pascual, S.; Colom, X. *Eur. Polym. J.* **2001**, *37*, 1457.
4. Jabrain, S. A.; Elizabeth, A. L. *J. Appl. Polym. Sci.* **1994**, *53*, 411.
5. Yang, R.; Liu, Y.; Yu, J.; Zhang, D. Q. *Polym. Eng. Sci.* **2008**, *48*, 2270.
6. Choi, B. H.; Balika, W.; Chudnovsky, A.; Pinter, G.; Lang, R. W. *Polym. Eng. Sci.* **2009**, *49*, 1421.
7. Welander, M. *Polymer* **1990**, *31*, 64.
8. Pinter, G.; Lang, R. W. *J. Appl. Polym. Sci.* **2003**, *90*, 3191.
9. Choi, B. H.; Chudnovsky, A.; Paradkar, R.; Michie, W. *Polym. Degrad. Stab.* **2009**, *94*, 859.
10. Shyichuk, A. V.; Stavychna, D. Y.; White, J. R. *Polym. Degrad. Stab.* **2001**, *72*, 279.
11. Nakamura, H.; Nakamura T.; Noguchi, T.; Imagawa, K. *Polym. Degrad. Stab.* **2006**, *91*, 740.
12. Popov, A. A.; Krisyuk, B. E.; Zaikov, G. Y. *Polym. Sci.* **1980**, *22*, 1501.
13. Popov, A. A.; Krisyuk, B. E.; Blinov, N. N.; Zaikov, G. E. *Eur. Polym. J.* **1981**, *17*,169.
14. Ricardo, B.; Marco-Aurelio, D. P. *Polym. Degrad. Stab.* **1993**, *40*, 53.
15. Axelson, D. E.; Levy, G. C.; Mandelkern, L. *Macromolecules* **1979**, *12*, 41.
16. Kaji, A.; Akitomo, Y.; Rano, M. *J. Polym. Sci. Part A Polym. Chem.* **1991**, *29*, 1987.
17. Müller, A. J.; María, L. A. *Prog. Polym. Sci.* **2005**, *30*, 559.

18. Keating, M. Y.; Lee, I. H.; Wong, C. S. *Thermochim. Acta* **1996**, *284*, 47.
19. Zhang, F. J.; Fu, Q.; He, T. B. *Polymer* **2002**, *43*, 1031.
20. Arnal, M. L.; Sanchez, J. J.; Müller, A. *J. Polymer* **2001**, *42*, 6877.
21. Fillon, B.; Wittmann, J. C.; Lotz, B.; Thierry, A. *J. Polym. Sci. Part B: Polym. Phys.* **1993**, *31*, 1383.
22. Wunderlich, B.; Dole, M. *J. Polym. Sci.* **1957**, *24*, 201.
23. Wunderlich, B.; Czornyj, G. *Macromolecules* **1977**, *10*, 906.
24. Randall, J. C. *Rev. Macromol. Chem. Phys.* **1989**, *C29*, 201.
25. Grant, M. D.; Paul, E. G. *J. Am. Chem. Soc.***1964**, *86*, 2984.
26. Lindeman, L. P.; Adams, J. Q. *Anal. Chem.* **1971**, *43*, 1245.
27. Randall, J. C.; Woodward, A. E.; Bovey, F. A. *ACS Symp. Ser.* **1980**, *142*, 93.
28. Fu, Q.; Chiu, F.; McCreight, K. W.; Guo, M. M.; Tseng, W. W.; Cheng, S. Z. D.; Keating, M. Y. *J. Macromol. Sci. Part B: Phys.* **1997**, *36*, 41.
29. Chen, F.; Shanks, R. A.; Amarasinghe, G. *Polym. Int.* **2004**, *53*, 1795.
30. Zhang, M. Q.; Wanke, S. E. *Polym. Eng. Sci.* **2003**, *43*, 1878.
31. Sabino, M. A.; Feijoo, J. L.; Muller, A. J. *Polym. Degrad. Stab.* **2001**, *73*, 541.
32. Rideal, G. R.; Padget, J. C. *Polym. Degrad. Stab.* **1976**, *57*, 1.
33. Gugumus, F. *Polym. Degrad. Stab.* **2000**, *67*, 35.
34. Zanasi, T.; Fabbri, E.; Pilati, F. *Polym. Test.* **2009**, *28*, 96.
35. Singh, A. *Radiat. Phys. Chem.* **1999**, *56*, 375.
36. Chattopadhyay, S.; Chaki, T. K.; Bhowmick, A. K. *J. Appl. Polym. Sci.* **2001**, *81*, 1936.
37. Ranadea, A.; Nayak, B. K.; Fairbrother C. D.; D'Souzaa, N. A. *Polymer* **2005**, *46*, 7323.